NANOMATERIALS

Uniform metal nanostructures with long-range order via three-step hierarchical self-assembly

10.1126/sciadv.1500751

Denise J. Erb,[1,2]* Kai Schlage, Ralf Röhlsberger[1,2]

Large-scale nanopatterning is a major issue in nanoscience and nanotechnology, but conventional top-down approaches are challenging because of instrumentation and process complexity while often lacking the desired spatial resolution. We present a hierarchical bottom-up nanopatterning routine using exclusively self-assembly processes: By combining crystal surface reconstruction, microphase separation of copolymers, and selective metal diffusion, we produce monodisperse metal nanostructures in highly regular arrays covering areas of square centimeters. In situ grazing incidence small-angle x-ray scattering during Fe nanostructure formation evidences an outstanding structural order in the self-assembling system and hints at the possibility of sculpting nanostructures using external process parameters. Thus, we demonstrate that bottom-up nanopatterning is a competitive alternative to top-down routines, achieving comparable pattern regularity, feature size, and patterned areas with considerably reduced effort. Intriguing assets of the proposed fabrication approach include the option for in situ investigations during pattern formation, the possibility of customizing the nanostructure morphology, the capacity to pattern arbitrarily large areas with ultrahigh structure densities unachievable by top-down approaches, and the potential to address the nanostructures individually. Numerous applications of self-assembled nanostructure patterns can be envisioned, for example, in high-density magnetic data storage, in functional nanostructured materials for photonics or catalysis, or in surface plasmon resonance–based sensing.

INTRODUCTION

In self-assembly, the size and shape of the resulting structures and the periodicity of structure patterns depend only on the inherent properties and internal interactions of the material that undergoes self-assembly, not on the capability of the tools that the material is processed with. Furthermore, self-assembly is a parallel process—all of the individual nanostructures in a pattern form simultaneously, and thus preparation can be extremely fast and fabrication time is independent of the sample size (*1*, *2*). Moreover there is one crucial advantage of nanostructure fabrication by self-assembly that is of particular interest from a fundamental scientific point of view: The nanostructures can be studied in situ during their formation, for example, regarding size- or shape-dependent characteristics or arising interactions and emerging collective phenomena. Among the diverse self-assembly processes, the microphase separation of block copolymers has attracted much attention because of the morphological variety of these systems. Diblock copolymer self-assembly has been successfully integrated into different nanopatterning and nanostructure fabrication routines. Numerous publications describe routines in which diblock copolymer films fulfill the function of masks, requiring removal of one copolymer block or subsequent removal of both blocks (*3*–*7*). Others demonstrate how selectivity toward the chemical components of a copolymer template can be used to assemble presynthesized nanoparticles (*8*, *9*). Only a few attempts have been made to develop nanopatterning procedures based on the selective wetting of metals deposited on diblock copolymer thin films. Initial works investigated mainly Au and Ag on polystyrene-*b*-poly(methyl methacrylate) (PS-*b*-PMMA) (*10*–*12*). They first demonstrated the principal possibility of growing self-assembling metal nanostructures on diblock copolymer templates and achieved granular nanostructures of nonuniform size and rather irregular shape. One recent publication indicates selective wetting of Co sputter deposited onto a polystyrene-*b*-poly(ethylene oxide) (PS-*b*-PEO) film but neither provides a quantitative analysis of nanostructure shapes nor investigates the effects of deposition conditions (*13*). None of the former studies were concerned with the long-range positional ordering of the metal nanostructures. With our contribution, we aim to establish the fabrication of highly ordered large-area arrays of monodisperse metal nanostructures using exclusively self-assembly processes. We show how the morphology of the metal nanostructure pattern can be adjusted via the molecular mass and composition of the diblock copolymer template. We demonstrate that uniform metal nanostructures with well-defined geometric shapes and smooth surfaces can be grown in a facile way by sputter deposition, and that readily accessible process parameters, such as the template temperature during metal deposition, can be used to influence the proportions of the metal nanostructures. The nanostructure fabrication routine that we bring forward here is a sequence of three self-assembly processes: (i) the spontaneous reconstruction of α-Al_2O_3 M-plane surfaces into nanoscale facets (*14*–*16*), (ii) the microphase separation in diblock copolymer thin films (*17*–*21*), and (iii) the growth of metal nanostructures on the chemically patterned surface of a diblock copolymer film (*11*, *22*). Our approach is hierarchical in that the pattern formed in one self-assembly process directs the pattern formation in the following process (see Fig. 1): First, an α-Al_2O_3 M-plane substrate is subject to high-temperature annealing, resulting in nanoscale faceting of the substrate surface (Fig. 1A). In the next step, a diblock copolymer thin film is spin-coated onto the nanofaceted α-Al_2O_3 substrate. Upon exposure to solvent vapor, the copolymer film undergoes microphase separation into uniformly shaped and evenly spaced domains of nanoscale size, consisting exclusively of one of the two copolymer blocks. Here, the α-Al_2O_3 substrate surface topography defines a pronounced preferential direction, inducing long-range order in the lateral positioning of the chemical domains within the diblock copolymer film (*23*, *24*).

[1]Deutsches Elektronen-Synchrotron (DESY), Notkestraße 85, 22607 Hamburg, Germany. [2]The Hamburg Centre for Ultrafast Imaging, Universität Hamburg, Luruper Chaussee 149, 22761 Hamburg, Germany.
*Corresponding author. E-mail: denise.erb@desy.de

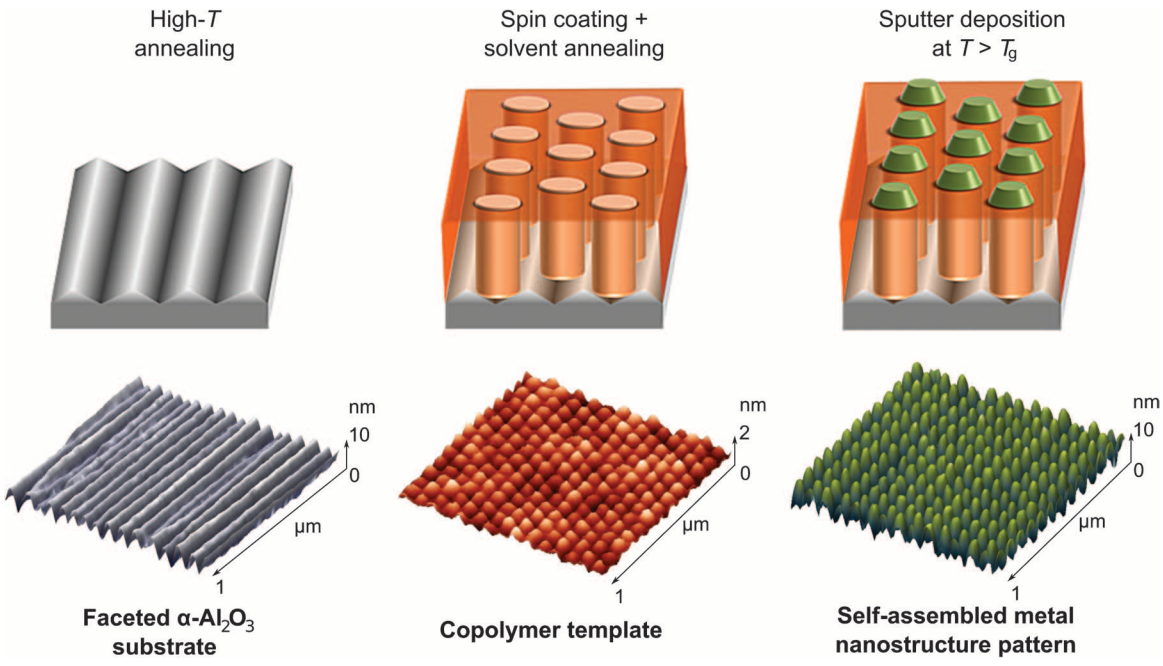

Fig. 1. Hierarchical self-assembly. Top: Sketch of the proposed nanostructure fabrication routine. Bottom: AFM topography scans of a nanostructured sample in subsequent stages. (**A**) Nanofaceted substrate obtained by high-temperature annealing of M-plane α-Al_2O_3. (**B**) Microphase-separated diblock copolymer template, with the lateral positioning of the chemical domains guided by the substrate topography. (**C**) Metal nanostructures formed during sputter deposition, following the chemical surface patterning presented by the diblock copolymer template.

Thus, the copolymer film presents a topographically almost flat but distinctly chemically structured surface of high regularity (Fig. 1B), which can be used as a template to grow a metal nanostructure pattern of the same morphology: Metals exhibiting a pronounced mobility contrast for surface diffusion on the two copolymer blocks will agglomerate on only one of the copolymer blocks (*22*). Moreover, shape equilibration to reduce interface energy proceeds significantly more slowly for nanometer-scale objects than for micrometer-sized structures (*25*). Thus, metal nanostructures can be quasi-stable in nonequilibrium shapes (for example, wires) following the chemical surface pattering of the diblock copolymer template (*11*, *12*). Thereby, the well-ordered two-dimensional (2D) chemical structuring of the template surface is transferred into a regular pattern of uniform 3D metal nanostructures (Fig. 1C). Such a hierarchically self-assembled sample system is depicted in Fig. 2: The atomic force microscopy (AFM) data show the metal nanostructure array grown on the diblock copolymer template supported by the nanofaceted substrate. Comparing the height profile of a copolymer template before metal deposition and the height profile of a deposited nanodot array evidences the selective growth of the metal on the PS domains.

RESULTS

Template fabrication: inducing long-range chemical order by substrate topography

Long-range lateral positional ordering of the chemical domains of the diblock copolymer thin film is induced by the topographical constraints that the nanofaceted surface morphology of the supporting substrate imposes on the configuration of the copolymer chains. The copolymer domains can only be deformed to a limited extent because of the condition to minimize free energy, that is, to maximize conformational entropy and to minimize domain interface energy (*17*, *18*, *26*). Therefore, during the microphase separation process upon solvent vapor annealing, the copolymer chains will orient and arrange in a way that accommodates the substrate facets while leading to minimal chain deformation.

The AFM topography micrographs presented in Fig. 3 compare the surface morphologies of PS-*b*-PMMA copolymer templates on polished planar silicon substrates with a native oxide layer (Fig. 3, A and C) to those of templates on faceted α-Al_2O_3 substrates (Fig. 3, B and D, the facet edges run from the top to the bottom of the images). The effect of the substrate topography on the lateral positional ordering of copolymer domains is demonstrated by two types of copolymer templates: a symmetric diblock copolymer forming lamellar domains (BCP-L) and an asymmetric diblock copolymer forming cylindrical PS domains in a PMMA matrix (BCP-C2). The height differences between the PS and the PMMA domains are, on average, less than 2 nm. For the symmetric diblock copolymer BCP-L on polished silicon substrates, we observed PS and PMMA alternating in meandering lamellar domains with a spacing of D = 48 nm (peak to peak). The asymmetric diblock copolymer BCP-C2 forms cylindrical domains of PS with a spacing of D = 83 nm (center to center) in a PMMA matrix. Orientation of the domains perpendicular to the film interfaces is ensured by film thicknesses $d < 0.5D$ (*26*). Although the polymer domains are very uniform in size, shape, and orientation, there is only short-range order in their lateral arrangement. On the faceted α-Al_2O_3 substrates, on the other hand, long-range positional ordering is obtained: For the symmetric diblock copolymer BCP-L, all lamellae align parallel to the substrate facets. The FFT of the topography shows sharp maxima at positions corresponding to the translational symmetry and lateral spacing of the chemical domains. For the asymmetric diblock copolymer BCP-C2, the PS domains are arranged in a 2D hexagonal

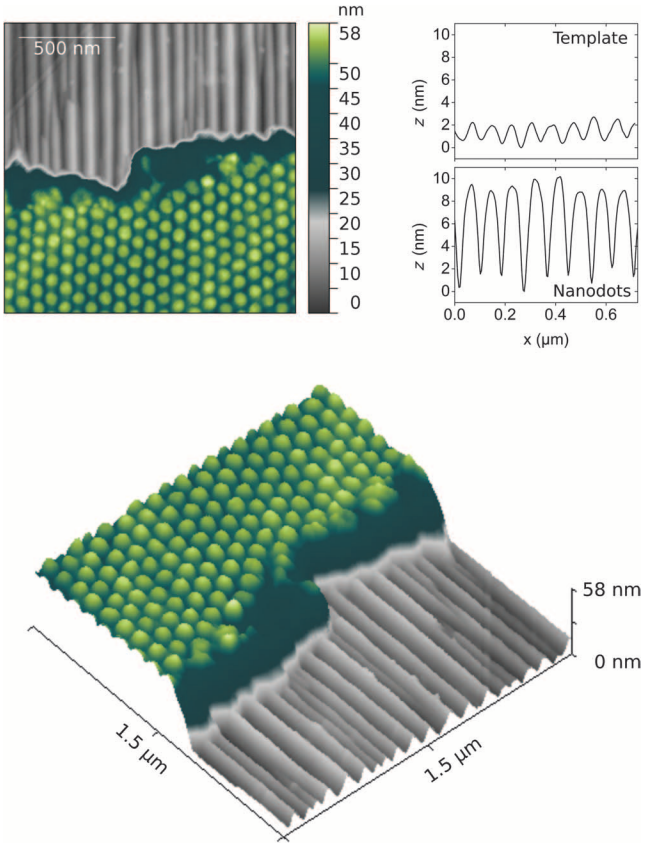

Fig. 2. AFM data illustrating the composition of self-assembled sample systems and the selective wetting of Fe on the copolymer template. (**A**) AFM micrograph of a sample system consisting of α-Al_2O_3 substrate, copolymer template, and Fe nanodots showing the exposed nanofaceted substrate in the upper half and the Fe nanodot array in the lower half. (**B**) AFM profiles of the nanodots and of the corresponding copolymer template before Fe deposition. In the template, the PS domains protrude slightly from the PMMA matrix. The increase in structure height after metal deposition evidences that Fe selectively grows on the PS domains. (**C**) Perspective view of (A).

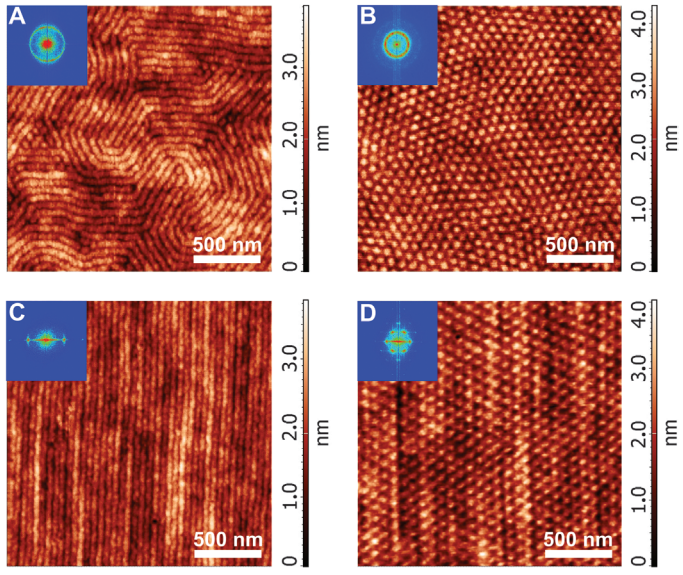

Fig. 3. Induction of long-range order in diblock copolymer templates by substrate topography. AFM topography micrographs comparing the chemical surface patterning of different diblock copolymer thin-film templates resulting from microphase separation. PS domains appear bright, and PMMA domains appear dark. Fast Fourier transforms (FFTs) of the respective topographies are shown. (**A** to **D**) Thin films of the diblock copolymers BCP-L (lamellar domain morphology) and BCP-C2 (cylindrical domain morphology) were prepared on planar SiO_x substrates (A and B) and on nanofaceted α-Al_2O_3 substrates (C and D). The uniaxially corrugated topography of the α-Al_2O_3 substrate induces long-range ordering in the lateral positioning of the chemical domains of the diblock copolymer thin film.

lattice, with the orientation of the (10) axis given by the orientation of the substrate facet edges. The respective FFT exhibits the sixfold symmetry of the hexagonal domain array with peak positions corresponding to the domain spacing. In both cases, the long-range precision of the lateral domain positioning is evidenced by the higher-order maxima in the FFTs. An influence of the substrate facet dimensions on the sizes of the chemical domains, i.e., a domain deformation, at the copolymer film surface is not observed. This results directly from the free energy minimization which maintains the equilibrium period D_0 of the copolymer.

This also results in the apparent tolerance of the diblock copolymer domain pattern to irregularities in the substrate surface topography. Perfect lateral domain ordering with uniform domain sizes and distances in the copolymer thin film does not require an α-Al2O3 substrate with a surface perfectly reconstructed into identical facets (see also Figs. 1 and 2). Facet dislocations are mostly ignored by the copolymer domains because strictly following every individual facet would necessitate many chain deformations. Rather, the copolymer domains are aligned along the direction given by the general orientation of the facets. Defects in the final domain pattern, which arise during the microphase separation process starting from the chemically disordered state, may be persistent if their removal requires spending more energy for mass transport than would be gained by achieving defect-free domain arrangement. Also, strong variations in height h and width L of individual facets within one substrate with typical standard deviations of $\sigma_h \approx 0.3h$ and $\sigma_L \approx 0.25L$, respectively, do not hinder the lateral domain ordering. Nevertheless, the average facet dimensions must meet two requirements.

It is crucial to match the average substrate facet height and the copolymer film thickness to achieve the optimum planarity of the copolymer film surface and the highest degree of positional ordering of the copolymer domains (see fig. S1). For our system, we found ratios of d/h between 3.5 and 7.5 to be the optimum ratio of film thickness d and facet height h. If d/h is too low, the surface of the diblock copolymer film will not be planar but will follow the corrugations of the faceted substrate surface. If d/h is too high, the guiding effect of the substrate topography is lost at the copolymer film surface and the obtained positional ordering of the chemical domains is of the same short range as for a planar SiO_x substrate.

Attention must also be paid to the ratio of the copolymer equilibrium domain period D_0 to the average substrate facet width L. For a constant d/h ratio, Rockford and co-workers (*23*) found that optimum lateral domain ordering was achieved for a ratio of $L/D_0 = 1 \pm 0.25$. Park and co-workers (*24*) achieved excellent long-range domain ordering up to ratios of $L/D_0 = 3$. The two studies significantly differ in that the molecular masses of the investigated copolymers were by factors of up to 80 larger in the first study (*23*) than in the second (*24*). For the samples

presented here, the ratio is $L/D_0 = 2.3$ for the copolymer with the lowest molecular mass (BCP-C1, $D_0 = 48$ nm) and $L/D_0 = 1$ for that with the highest (BCP-C2, $D_0 = 83$ nm) (see fig. S2, B and C, respectively). In our study, we find copolymers of lower molecular mass, that is, of smaller domain period $D_0 < 50$ nm, showing a higher degree of lateral domain ordering and a weaker dependence of the degree of lateral domain ordering on the L/D_0 ratio. This indicates that defect-free long-range lateral domain ordering is more facile and more robustly achieved in low-mass copolymers because of the higher mobility of shorter polymer chains.

Templated metal nanostructure growth: Ex situ observations by AFM

To grow metal nanostructure patterns by selective wetting, different metals were sputter deposited onto diblock copolymer templates at various temperatures and deposition rates (see Fig. 4). For the inert metal Au, we observed the formation of small metal clusters, with their positioning almost unaffected by the template for a wide range of conditions. In agreement with earlier findings by Lopes and co-worker (*11*, *12*), we observed a slight selectivity of Ag toward the PS domains: Mostly, cluster formation dominated the Ag growth, but in some rare cases, Ag deposition above the glass transition temperature of the copolymer template resulted in nanostructures of comparatively irregular shapes. Templated Ag nanostructure growth with precise reproduction of the template morphology may be found for a narrow range of deposition conditions. In contrast, the reactive metals Fe, Pt, and Ni readily formed uniform and well-separated nanostructures for almost all deposition conditions. The metals selectively grow on the PS domains, reproducing the domain shapes and arrangement given by the chemical surface pattern of the templates. The disparate behavior of inert and reactive metals is attributed to a different balance of metal/metal and metal/polymer interactions (*11*, *12*). Effective selective wetting requires a suitable balance between the metal-metal sticking coefficient and the so-called mobility contrast, which is the difference in the diffusivity of the metal on the chemically distinct domains of the copolymer template (*22*). The diffusivity depends on the type of adsorption interaction between metal and polymer, with physisorption indicating weak interaction and higher diffusivity and with chemisorption resulting in strong interaction and lower diffusivity. The type of adsorption interaction between a metal and a polymer surface is specific for each material combination and can be influenced by the preparation conditions of the polymer film, which can cause different groups of the polymer, that is, potential interaction sites for the metal, to be expressed at the film surface. In general, inert metals are expected to mainly adsorb to polymers by physisorption because of their chemical inertness. Reactive metals are generally more likely to interact with polymers by chemisorption and can exhibit strong chemical affinity toward certain polymers (*27*, *28*). For Au and Ag deposited onto the PS-*b*-PMMA surface, we observe little to no preferred adsorption of the metal on one of the components of the copolymer template. For Fe, Pt, and Ni, however, the chemical contrast between the PS and the PMMA translates into a contrast in mobility, with lower diffusivity on the PS domains and with higher diffusivity on the PMMA domains. This mobility contrast effectively results in the metal atoms clearing the PMMA domains and agglomerating on the PS domains. Thus, 3D metal nanostructures form, reproducing the morphology of the chemical patterning of the template.

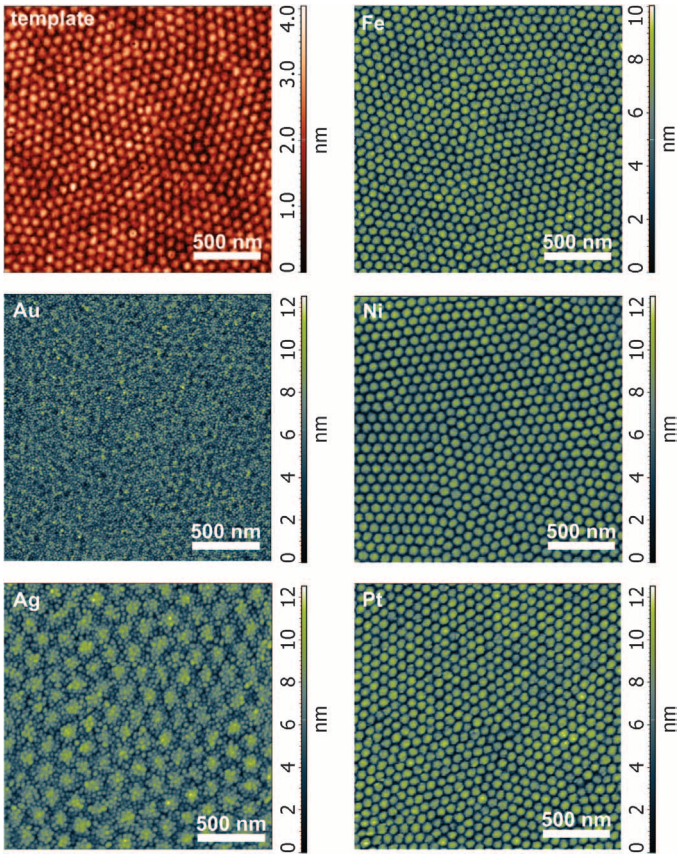

Fig. 4. Wetting selectivity of different metals on PS-*b*-PMMA templates. Au, Ag, Fe, Ni, and Pt were grown on diblock copolymer templates with cylindrical morphology (BCP-C2) on planar SiO_x substrates. Whereas Au and Ag form very small clusters all over the template surface, the other metals form smooth and well-separated nanostructures reproducing the chemical patterning of the template surface.

Here, the nominal thickness of the deposited metals ranges from 0.3 nm [about 1.5 monolayers (ML)] to 2.1 nm (about 10 ML). Within this range, we invariably grow uniform and well-separated nanostructures by template self-assembly. From a nominal thickness of about 3 nm (about 15 ML) onward, we observe that the metal nanostructures begin to merge and finally form a closed metal film.

Given that a metal reproduces the template pattern well, control over the shape, size, and lateral arrangement of the metal nanostructures is obtained via control over the morphology of the diblock copolymer template: The shapes of the metal nanostructures follow the copolymer domain morphology at the film surface, as given by the volume fractions of the copolymer blocks. When using self-assembly processes for nanostructure fabrication, the shapes and arrangements of the nanostructures cannot be designed as arbitrarily as when using lithographical methods. Nevertheless, domain morphologies of block copolymers cover a large range of scientifically and technologically relevant structures and patterns. Diblock copolymers with their cylindrical and lamellar domains allow for growing nanostructures in the shape of hexagonally arranged dots and antidots or parallel wires. Triblock copolymers have an even richer morphological phase diagram containing, among many others, concentric domains, combinations of lamellar and spherical domains, or morphologies with square symmetry (*29*–*31*). Block copolyelectrolytes, consisting of one charged block and one neutral block, allow for additional electrostatic control of the domain morphology, for example, of the ratio of the diameter of cylindrical domains to the spacing of cylindrical domains (*32*).

Dot-shaped or wire-like metal nanostructures with a high degree of regularity in lateral positioning can be prepared on diblock copolymer templates with cylindrical or lamellar domain morphology, respectively, on nanofaceted α-Al_2O_3 substrates, as shown in Fig. 5 (see also fig. S2 for AFM topographies of larger sample areas). Here, the periodic substrate topography guides the chemical surface patterning of the diblock copolymer template, which is, in turn, transferred into a highly regular pattern of 3D metallic nanostructures. The metal nanostructures can be scaled down or up in size by providing templates with desired sizes of the copolymer domains (ranging from less than 5 nm to a few hundred nanometers), as determined by the molecular mass of the diblock copolymer. Both the volume fractions of the individual blocks and the total molecular mass can be well controlled in the synthesis of a diblock copolymer. Comparing Fig. 5, B and D, demonstrates down-scaling of hexagonally arranged Fe nanodots by reducing the PS domain size and spacing from 58 to 31 nm in diameter and from 83 to 48 nm in center-to-center distance via choosing diblock copolymers of the appropriate molecular mass. This corresponds to increasing the pattern density from 0.1 to 0.3 Tbit/inch^2, thus approaching the density of contemporary hard disk drive storage (*33*). Pattern densities of 10 Tbit/inch^2 with nanodots of 3 nm in diameter have been demonstrated in copolymer templates (*24*) but have not been transferred to metallic nanostructure patterns in the respective study.

Because of the parallel nature of self-assembly processes, increasing the sample area means increasing the rate of nanopatterning. In our laboratory-scale study, we achieved metal nanostructure patterning rates of about 1 cm^2/hour. We discuss possible approaches to further increasing the patterning rate and sample throughput in the Supplementary Materials.

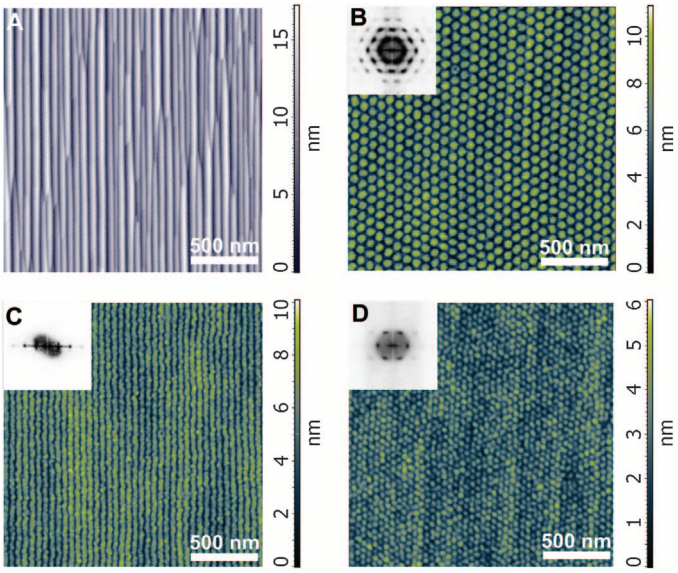

Fig. 5. Highly ordered self-assembled metal nanostructure patterns. (**A** to **D**) Diblock copolymer templates on nanofaceted α-Al_2O_3 substrates (A) exhibit a highly regular chemical surface pattern on which uniform dot-shaped (B and D) or wire-like (C) nanostructures with highly ordered lateral positioning are grown. Comparing the nanostructures grown on templates of copolymers BCP-C1 and BCP-C2 with identical domain morphology but different domain sizes illustrates how the nanostructure size can be scaled via the copolymer molecular mass. Moreover, the nanostructure pattern can be reversed by reversing the volume fractions of PS and PMMA in the diblock copolymer to produce antidots. See fig. S2 for large-area AFM topography scans.

Influence of template temperature on the self-assembly of Fe nanodot patterns: High-resolution morphological characterization by in situ grazing incidence small-angle x-ray scattering

Because of the temperature dependence of surface diffusion processes and of the time scale for shape equilibration (*25*), an effect of the template temperature on the resulting nanostructure morphology is expected. AFM micrographs, however, are compromised by the probe size and by the convolution of the nanostructure shape with the tip shape and thus hardly allow for unambiguous determination of the nanostructure shape. Scanning electron microscopy measurements would be hindered by the fact that the sample surface is not continuously conductive, and depositing a conductive layer on top obscures the details of the nanostructure morphology. Moreover, it is not trivial to realize in situ microscopy measurements on nanostructures during growth. To observe the size, shape, and lateral positioning of iron nanostructures during their formation at different template temperatures, we performed in situ grazing incidence small-angle x-ray scattering (GISAXS) during iron sputter deposition. Two hexagonal arrays of iron nanodots were grown on BCP-C2 templates on nanofaceted α-Al_2O_3 at room temperature and at about 170°C, respectively. The deposition processes were regularly interrupted to obtain GISAXS patterns. At an incidence angle of 0.3° and at a cross-section of the x-ray beam of about 0.1 mm × 0.1 mm, the sample area illuminated by the x-ray beam is about 20 mm in length and 0.1 mm in width. Because the investigated samples have a maximum size of 15 mm × 15 mm, the morphology found in the illuminated area is considered to be representative of the entire sample area.

GISAXS data were evaluated using IsGISAXS software (*34*), yielding values for the lateral nanostructure arrangement and for the development of the nanostructure size and shape during growth. Figure 6 shows exemplary experimental data with corresponding simulations for both iron nanodot arrays (please refer to figs. S3 and S4 for data and simulations for all deposition stages). Analogous information is given for one nanodot array grown in continuous deposition at about 170°C without interruptions for scattering data acquisition; the GISAXS pattern was recorded at the end of the deposition process.

The fact that no distributions in particle dimensions or arrangement had to be assumed for the simulations demonstrates the outstanding morphological uniformity and positional regularity of nanostructure arrays prepared via the proposed routine. All scattering patterns evidence a hexagonal arrangement of nanodots with a lattice constant of 83 nm as given by the diblock copolymer template. Among the form factors implemented in the simulation program, truncated cones provided the best possible approximation to the average nanodot shape. Given the high degree of uniformity of the nanodots, it is valid to consider this average particle shape to correspond well to the shape of an individual nanodot. However, no satisfying agreement between simulation and experimental data could be found for the early stages of nanodot growth at 170°C, indicating that here the assumed form factor does not correspond well to the actual nanodot shape. Geometrical parameters describing the nanodot shape as extracted from simulations for all stages of growth are summarized in Fig. 7. Under both growth conditions, the base angle and the ratio of height to base radius remain roughly constant during growth, irrespective of the different deposition rates. The quantitative effect of the template temperature on the nanodots, however, is

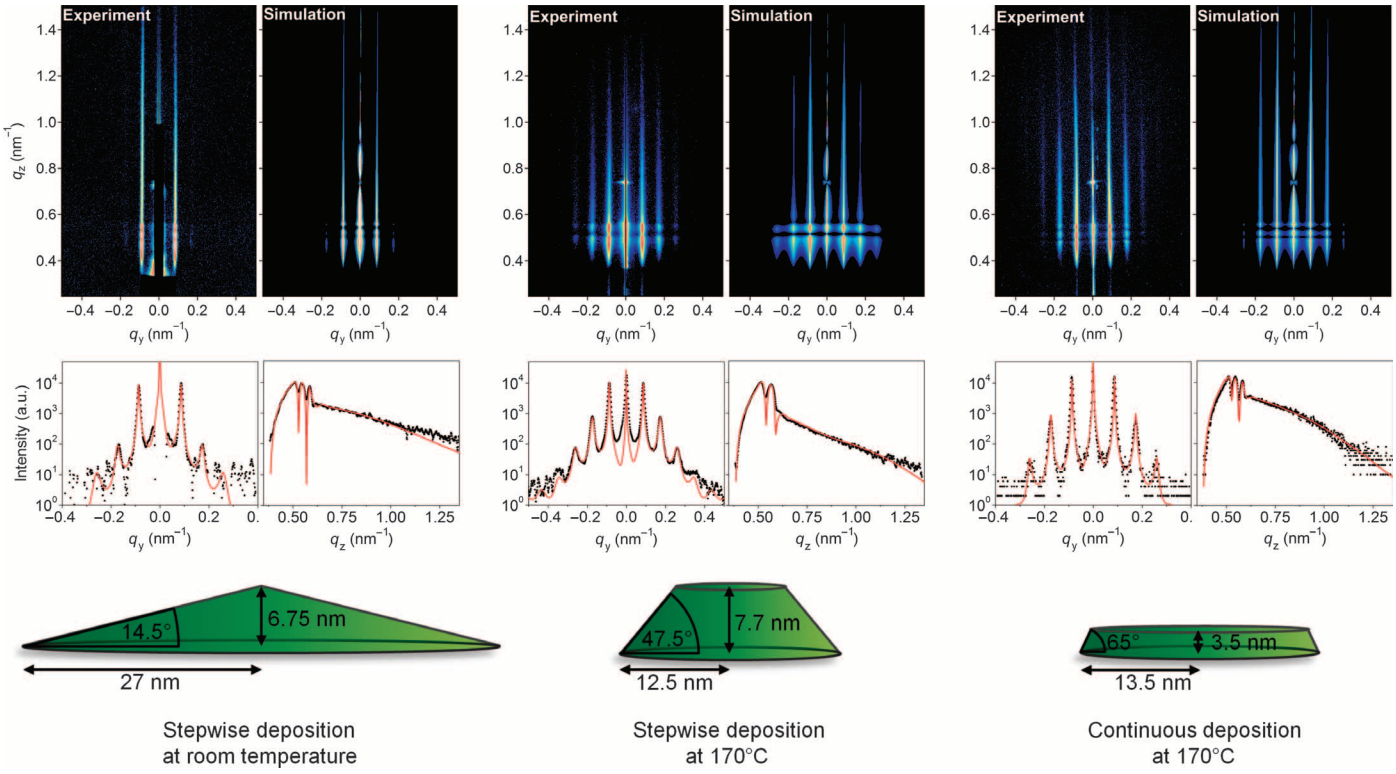

Fig. 6. Morphological characterization by in situ GISAXS. The morphologies of self-assembled Fe nanodots in hexagonal arrays forming under different metal deposition conditions were determined with high accuracy by simulating GISAXS patterns recorded in situ during growth. Top: GISAXS scattering pattern and corresponding 2D simulations. Middle: Horizontal and vertical sections through the experimental and simulated scattering patterns as indicated above. Bottom: Sketches depicting the resulting proportions of the nanodots as deduced from the simulations. See figs. S3 and S4 for GISAXS data and simulations of all stages of growth. a.u., arbitrary units.

remarkable: At any given deposition stage, the aspect ratio of height to base radius is about 0.65 for the nanodots growing at 170°C and only about 0.25 for the nanodots growing at room temperature. The base angle is more than three times as large for the nanodots growing at 170°C as compared to the sample at room temperature; for continuous Fe deposition, the angle is even more than four times larger. In the sample grown at room temperature, the nanodots eventually extend their radius over the radius of the PS domains of about 29 nm, rather than growing more in height. Apparently, the nanodot proportions strongly depend on the template temperature because of its effect on the iron atoms' kinetics on the template surface: At room temperature, the equilibration time of nanometer-scaled bodies can easily reach the range of months (*22*, *25*). Consequently, surface area minimization of the nanodots is impeded, and growth at room temperature results in wide, flat nanodots. At higher template temperatures, the mobility of iron atoms and clusters is enhanced, and the equilibration time can be reduced to the range of a few hours. Thus, compact iron nanodots with lower surface-to-volume ratio form. The very different nanodot proportions resulting from different growth conditions (see Fig. 6) hint at an approach to shaping self-assembling nanostructures by controlling external process conditions.

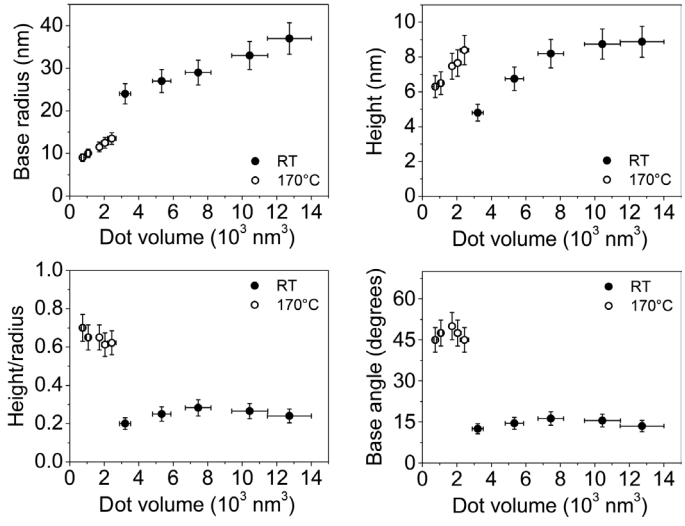

Fig. 7. Evolution of nanodot proportions during growth. The geometrical parameters describing the proportions of Fe nanodots forming at 170°C and at room temperature (RT), respectively, were extracted from simulations of in situ GISAXS data (see also figs. S3 and S4).

DISCUSSION

Our novel routine brings together two approaches in nanostructure fabrication: The directed microphase separation of diblock copolymer films on nanostructured substrate surfaces was combined with the self-assembly of metal atoms on microphase-separated diblock copolymer templates. Exclusive use of self-assembly processes

eliminates the requirement for complex devices for lithographical nanopatterning and allows for in situ studies throughout the entire procedure. After our hierarchical self-assembly routine, diverse metal nanostructure patterns with a high degree of morphological uniformity and positional regularity can be prepared on large sample areas. Moreover, our findings inferred from in situ GISAXS during Fe nanodot growth indicate that the proportions of nanostructures can be influenced via deposition conditions such as the template temperature. Furthermore, size limitations of top-down nanopatterning approaches could be overcome by using diblock copolymers of lower molecular mass (*24*), which potentially allow scaling of the metal nanostructure sizes down to diameters below 5 nm. The option to perform in situ experiments on large arrays of uniform metal nanostructures can significantly facilitate the study of size- and shape-dependent optical, electrical, magnetic, or plasmonic properties and their interrelations. The outstanding uniformity of the nanostructures should allow for identifying interactions among them and for studying nanostructure properties accurately without the need to isolate individual nanostructures from the ensemble. The morphological quality of the nanostructures also encourages extending the nanopatterning to morphologies provided by triblock copolymers, which comprise, among many others, morphologies with square symmetry or honeycomb patterning (*29*–*31*). The proposed routine is fast, facile, versatile, and economic. It offers exciting possibilities: arbitrarily covering large surface areas with various patterns of customizable identical nanostructures, achieving ultrahigh structure densities, or addressing individual nanostructures in a highly ordered array (*24*). High-density magnetic recording, surface plasmon resonance–based sensing, or materials for catalysis may be among the future applications of these self-assembling nanopatterned composite systems.

MATERIALS AND METHODS

Sample preparation

Wafers of polished M-plane α-Al_2O_3 were purchased from CrysTec GmbH, cleaned for 15 min in an ultrasonic bath of acetone at 50°C, and annealed in air in a chamber furnace at 1300° to 1400°C for 8 to 10 hours. Lamellae-forming (symmetric) and cylinder-forming (asymmetric) PS-*b*-PMMA diblock copolymers were purchased from Polymer Source Inc. The diblock copolymers were dissolved in toluene at concentrations ranging from 8 to 12 mg/ml and spin-coated onto the α-Al_2O_3 substrates. The copolymer thin films were then dried for 2.5 hours at 50°C in air. Microphase separation was accomplished by solvent annealing in saturated acetone vapor at room temperature for 2 to 3 hours. Metal nanostructures were grown on the copolymer templates by magnetron sputter deposition, using a custom-made UHV chamber at constant template temperatures ranging from room temperature to about 170°C (see also tables S1 and S2).

AFM and GISAXS data acquisition

AFM topography micrographs were recorded ex situ with an NT-MDT Solver NEXT scanning probe microscope in noncontact mode using HA_NC Etalon probes. For in situ GISAXS experiments performed at the synchrotron x-ray source PETRA III, the sputter deposition chamber was installed at beamline P01, and measurements were carried out at a wavelength of 14.4 keV. GISAXS patterns were recorded using a MAR345 image plate detector. The sample-detector distance of 5230 mm was bridged by an evacuated flight tube to reduce scattering in air.

SUPPLEMENTARY MATERIALS

Supplementary material for this article is available at http://advances.sciencemag.org/cgi/content/full/1/10/e1500751/DC1

Fig. S1. AFM micrographs illustrating the dependence of the degree of lateral domain ordering on the ratio of diblock copolymer film thickness to substrate facet height.

Fig. S2. Large-area AFM scans of highly ordered metal nanostructure patterns.

Fig. S3. Experimental data and simulations of GISAXS patterns for hexagonal Fe nanodot array growing at room temperature.

Fig. S4. Experimental data and simulations of GISAXS patterns for hexagonal Fe nanodot array growing at 170°C.

Table S1. Compositional properties of the diblock copolymers used.

Table S2. List of apparatus and duration of individual process steps. Discussion of nanopattern yield.

REFERENCES AND NOTES

1. J. D. Halley, D. A. Winkler, Consistent concepts of self-organization and self-assembly. *Complexity* **14**, 10–17 (2008).
2. J. J. Ramsden, in *Advanced Nanomaterials*, K. E. Geckeler, H. Nishide, Eds. (Wiley VCH, Weinheim, 2010), pp. 767–790.
3. S. Xiao, X. Yang, E. W. Edwards, Y.-H. La, P. F. Nealy, Graphoepitaxy of cylinder-forming block copolymers for use as templates to pattern magnetic metal dot arrays. *Nanotechnology* **16**, S324–S329 (2005).
4. E. B. Gowd, B. Nandan, M. K. Vyas, N. C. Bigall, A. Eychmüller, H. Schlörb, M. Stamm, Highly ordered palladium nanodots and nanowires from switchable block copolymer thin films. *Nanotechnology* **20**, 415302–415311 (2009).
5. B. Nandan, E. B. Gowd, N. C. Bigall, A. Eychmüller, P. Formanek, P. Simon, M. Stamm, Arrays of inorganic nanodots and nanowires using nanotemplates based on switchable block copolymer supramolecular assemblies. *Adv. Funct. Mater.* **19**, 2805–2811 (2009).
6. Y. S. Jung, J. H. Lee, J. Y. Lee, C. A. Ross, Fabrication of diverse metallic nanowire arrays based on block copolymer self-assembly. *Nano Lett.* **10**, 3722–3726 (2010).
7. K. Schlage, S. Couet, S. V. Roth, U. Vainio, R. Rüffer, M. M. Abul Kashem, P. Müller-Buschbaum, R. Röhlsberger, The formation and magnetism of iron nanostructures on ordered polymer templates. *New J. Phys.* **14**, 043007–043019 (2012).
8. E. B. Gowd, B. Nandan, N. C. Bigall, A. Eychmüller, P. Formanek, M. Stamm, Hexagonally ordered arrays of metallic nanodots from thin films of functional block copolymers. *Polymer* **51**, 2661–2667 (2010).
9. A. Horechyy, N. E. Zafeiropoulos, B. Nandan, P. Formanek, F. Simon, A. Kiriy, M. Stamm, Highly ordered arrays of magnetic nanoparticles prepared *via* block copolymer assembly. *J. Mater. Chem.* **20**, 7734–7741 (2010).
10. T. L. Morkved, P. Wiltzius, H. M. Jaeger, D. G. Grier, T. A. Witten, Mesoscopic self-assembly of gold islands on diblock-copolymer films. *Appl. Phys. Lett.* **64**, 422–424 (1994).
11. W. A. Lopes, H. M. Jaeger, Hierarchical self-assembly of metal nanostructures on diblock copolymer scaffolds. *Nature* **414**, 735–738 (2001).
12. W. A. Lopes, Nonequilibrium self-assembly of metals on diblock copolymer templates. *Phys. Rev. E* **65**, 031606–031619 (2002).
13. E. Metwalli, V. Körstgens, K. Schlage, R. Meier, G. Kaune, A. Buffet, S. Couet, S. V. Roth, R. Röhlsberger, P. Müller-Buschbaum, Cobalt nanoparticles growth on a block copolymer thin film: A time-resolved GISAXS study. *Langmuir* **29**, 6331–6340 (2013).
14. C. Herring, Some theorems on the free energies of crystal surfaces. *Phys. Rev.* **82**, 87–91 (1951).
15. J. R. Heffelfinger, C. B. Carter, Mechanisms of surface faceting and coarsening. *Surf. Sci.* **389**, 188–200 (1997).
16. V. A. Shchukin, D. Bimberg, Spontaneous ordering of nanostructures on crystal surfaces. *Rev. Mod. Phys.* **71**, 1125–1171 (1999).
17. F. S. Bates, G. H. Fredrickson, Block copolymer thermodynamics: Theory and experiment. *Annu. Rev. Phys. Chem.* **41**, 525–557 (1990).
18. F. S. Bates, Polymer-polymer phase behavior. *Science* **251**, 898–905 (1991).
19. C. Sinturel, M. Vayer, M. Morris, M. A. Hillmyer, Solvent vapor annealing of block copolymer thin films. *Macromolecules* **46**, 5399–5415 (2013).
20. M. J. Fasolka, A. M. Mayes, Block copolymer thin films: Physics and applications. *Annu. Rev. Mater. Res.* **31**, 323–355 (2001).
21. Y. Xuan, J. Peng, L. Cui, H. Wang, B. Li, Y. Han, Morphology development of ultrathin symmetric diblock copolymer film via solvent vapor treatment. *Macromolecules* **37**, 7301–7307 (2004).
22. A. Gopinathan, Kinetic self-assembly of metals on copolymer templates. *Phys. Rev. E* **71**, 041601–041608 (2005).
23. L. Rockford, Y. Liu, P. Mansky, T. P. Russell, M. Yoon, S. G. J. Mochrie, Polymers on nanoperiodic, heterogeneous surfaces. *Phys. Rev. Lett.* **82**, 2602–2605 (1999).

24. S. Park, D. H. Lee, J. Xu, B. Kim, S. W. Hong, U. Jeong, T. Xu, T. P. Russell, Macroscopic 10-terabit–per–square-inch arrays from block copolymers with lateral order. *Science* **323**, 1030–1033 (2009).
25. N. Combe, P. Jensen, A. Pimpinelli, Changing shapes in the nanoworld. *Phys. Rev. Lett.* **85**, 110–113 (2000).
26. M. J. Fasolka, P. Banerjee, A. M. Mayes, G. Pickett, A. C. Balazs, Morphology of ultrathin supported diblock copolymer films: Theory and experiment. *Macromolecules* **33**, 5702–5712 (2000).
27. T. Strunskus, M. Grunze, G. Kochendoerfer, C. Wöll, Identification of physical and chemical interaction mechanisms for the metals gold, silver, copper, palladium, chromium, and potassium with polyimide surfaces. *Langmuir* **12**, 2712–2725 (1996).
28. F. Faupel, R. Willecke, A. Thran, Diffusion of metals in polymers. *Mater. Sci. Eng.* **22**, 1–55 (1998).
29. J. Park, S. Jang, J. K. Kim, Morphology and microphase separation of star copolymers. *J. Polym. Sci. B* **53**, 1–21 (2015).
30. V. Abetz, in *Encyclopedia of Polymer Science and Technology* (John Wiley & Sons Inc., New York, 2002).
31. Y. Matsushita, A. Takano, K. Hayashida, T. Asari, A. Noro, Hierarchical nanophase-separated structures created by precisely-designed polymers with complexity. *Polymer* **50**, 2191–2203 (2009).
32. C. E. Sing, J. W. Zwanikken, M. Olvera de la Cruz, Electrostatic control of block copolymer morphology. *Nat. Mater.* **13**, 694–698 (2014).
33. Toshiba, press release (8 August 2015); http://toshiba.semicon-storage.com/us/company/taec/news/news-topics/2015/02/topics-20150224-1.html
34. R. Lazzari, *IsGISAXS*: A program for grazing-incidence small-angle X-ray scattering analysis of supported islands. *J. Appl. Crystallogr.* **35**, 406–421 (2002).

Acknowledgments: We thank H.-C. Wille and F.-U. Dill at beamline P01, PETRA III, for their support in preparing and conducting the GISAXS experiments. **Funding:** This work was financed by Deutsches Elektronen-Synchrotron (DESY) as an in-house research project without third-party funding contributions. **Author contributions:** K.S. and D.J.E. conceived the experiment, and K.S. constructed the in situ GISAXS experimental setup. D.J.E. and K.S. fabricated the samples, perfomed the measurements, and analyzed the data. All authors wrote the paper. R.R. and K.S. advised on the experiments. **Competing interests:** The authors declare that they have no competing interests. **Data and materials availability:** All data needed to evaluate the conclusions in the paper are present in the paper and/or the Supplementary Materials. Additional data related to this paper may be requested from the authors.

Submitted 10 June 2015
Accepted 30 August 2015
Published 6 November 2015
10.1126/sciadv.1500751

Citation: D. J. Erb, K. Schlage, R. Röhlsberger, Uniform metal nanostructures with long-range order via three-step hierarchical self-assembly. *Sci. Adv.* **1**, e1500751 (2015).

ScienceAdvances
AAAS

Uniform metal nanostructures with long-range order via three-step hierarchical self-assembly

Denise J. Erb, Kai Schlage and Ralf Röhlsberger (November 6, 2015)

Sci Adv 2015, 1:.
doi: 10.1126/sciadv.1500751